Behavior of Interfacial Oxide during Diffusion Bonding of Aluminum Alloys and Its Influence on Joint Strength†

Keiko KOTANI*, Kenji IKEUCHI**, and Fukuhisa MATSUDA***

Abstract

In order to investigate the interfacial phase formed during the diffusion bonding of the aluminum alloy and to discuss its influence on the bond strength, TEM observations have been carried out for joint interfaces of commercial aluminum alloys: Al-Mg-Si alloy 6063, Al-Mg alloy 5005, and Al-Zn-Mg alloy 7N01. At the joint interfaces of these alloys, amorphous oxide films were observed, and they were altered gradually to crystalline oxide particles, as the bonding temperature was increased. The bonding temperature at which the amorphous oxide film disappeared lowered with increasing the Mg content. As the area occupied by the amorphous oxide film was decreased, the tensile strength of the joints of all the alloys increased significantly, suggesting that the amorphous oxide was a major factor that decreased the bond strength. At all bonding temperatures employed, the crystalline oxides at the joint interfaces of 6063 and 7N01 alloys were identified as Al_2MgO_4 and MgO, respectively. In contrast, at the joint interface of 5005 alloy, both the crystalline oxides were observed depending on bonding temperature T_W; i.e., Al_2MgO_4 and MgO at T_W below 853 K, and Al_2MgO_4 at T_W above 853 K. In addition, particulate intermetallic compounds much larger than the crystalline oxides were precipitated preferentially at the joint interface even compared with the grain boundary. These precipitates observed in the joints of 6063 and 7N01 alloys were identified as Mg_2Si and $MgZn_2$, respectively. Although the fracture morphology of the joint suggested that these precipitates acted as initiation sites of dimples in tensile tests, it can be considered that they have much less influence on the bond strength than the amorphous oxide film, since solution treatments for dissolving these precipitates resulted in only slight improvement in the tensile strength.

KEY WORDS: (Diffusion Bonding) (Aluminum Alloy) (Oxide Film) (TEM Observation) (Bond Strength) (Magnesium) (Al_2MgO_4) (MgO)

1. Introduction

In diffusion bonding of aluminum and its alloys, it has been generally accepted that the stable superficial oxide film remains at the bond line even at bonding temperatures close to the melting point of the alloy and has very harmful effects on the bond strength[1-2]. Through the TEM observation of the joint interface of commercial aluminum alloys bonded at temperatures around 873 K[2-7], we have found that (1) the morphology of oxide at the joint interface is significantly affected by the alloying element, (2) the alloying element Mg can alter the morphology of the interfacial oxide from amorphous films to crystalline particles, whereas alloying elements of Si, Zn, and Cu have almost no influence on the morphology of interfacial oxide, and (3) precipitates of intermetallic compounds which are much larger than the crystalline oxide particle are formed preferentially at the joint interface of most of the commercial aluminum alloys. This study is aimed at investigating the influences of these interfacial phases on the bond strength of the commercial aluminum alloy. For this, three commercial aluminum alloys with different Mg content, viz. Al-Mg-Si alloy 6063, Al-Mg alloy 5005, and Al-Zn-Mg alloy 7N01 have been diffusion-bonded at temperatures ranging from 703 to 873 K, and factors influencing the joint strength have been discussed on the basis of TEM and SEM observations of the interfacial phases and fracture morphology after tensile tests.

2. Experimental Details

The base metals employed were commercial aluminum alloys: Al-Mg-Si alloy 6063, Al-Mg alloy 5005, and Al-Zn-Mg alloy 7N01 with chemical compositions as shown in **Table 1**. The specimen for diffusion bonding was a round bar 14 mm in diameter

† Received on 8 December 1997.

* Joint Researcher (Industrial Research Institute of Aichi Prefecture)

** Professor

*** Professor Emeritus(Presently at Power Engineering and Inspection Corporation)

Transactions of JWRI is published by Joining and Welding Reseach Institute of Osaka University, Ibaraki, Osaka 567, Japan.

Table 1 Chemical compositions of the base metals (mass%).

Alloy	Si	Fe	Cu	Mn	Mg	Cr	Zn	Ti	Al
Al-Mg-Si (6063)	0.41	0.19	0.02	0.01	0.54	0.02	0.02	0.02	Bal.
Al-Mg (5005)	0.06	0.15	0.01	0.01	0.80	0.01	0.01	0.01	Bal.
Al-Zn-Mg (7N01)	0.10	0.16	0.09	0.43	1.15	0.21	4.57	0.03	Bal.

Table 2 Diffusion-bonding parameters.

Alloy	T_W(K)	P_W(MPa)
Al-Mg-Si (6063)	793-893	4.0(at T_W=793K)- 1.0(at T_W=893K)
Al-Mg (5005)	793-873	3.0(at T_W=793K)- 1.0(at T_W=873K)
Al-Zn-Mg (7N01)	703-893	6.0(at T_W=703K)- 1.0(at T_W=893K)

and 37 mm in length. The faying surface was finished by turning in a lathe followed by electropolishing in an ethanol solution containing 10 vol% perchloric acid at 253 K and 18 V. The diffusion bonding was carried out in a vacuum of 10^{-2} Pa using an apparatus similar to that reported in a previous paper[8]. Bonding temperature T_W and bonding pressure P_W are listed in **Table 2**. Bonding time t_W was 1.8 ks for all joints bonded in this investigation. The specimen for the TEM observation was prepared as follows. Firstly a thin plate about 1 mm in thickness including the joint interface was cut at an angle of 90° and 30° with the joint interface, and then ground on 1500 grade emery paper to a thickness of about 100 μm. The plate was further thinned by electropolishing using a twin jet polishing apparatus. The electrolyte used was a solution of 5 vol% perchloric acid in methanol. The electropolishing temperature and voltage were 253 K and 18 V, respectively. The plate was finally thinned by Ar ion thinning. TEM observations were carried out at an acceleration voltage of 200 kV. Interfacial phases were identified by selected area or micro-beam diffraction techniques. The bond strength was estimated from tensile strength at room temperatures. The tensile test was carried out at a strain rate of 5.5×10^{-4} s^{-1} using a specimen 8 mm in diameter and 30 mm in gauge length.

3. Experimental Results and Discussion

3.1 TEM observation of joint interfaces of 5005, 6063, and 7N01 alloys

The effect of bonding temperature on the morphology of the interfacial oxide of the 6063 alloy joint is shown in **Fig. 1**. The joint interfaces were tilted by 35° to the incident beam in Fig. 1. At a bonding temperature of 793 K, continuous films were observed over almost the whole area of the joint interface as shown in Fig. 1(a). These interfacial continuous films can be regarded as amorphous oxides originating from the oxide film that existed on 6063 alloy surfaces; for (1) diffuse halo patterns were observed in the SAD pattern taken from areas involving the joint interface shown in Fig. 1(a), (2) the contrast of the TEM image of this continuous film was hardly influenced by tilting the specimen, and (3) O, Al, and Mg were detected by Auger electron analysis from the fractured surface of a joint, when the joint interface was similar to that shown in Fig. 1(a). As can be seen from Fig. 1(b), at a bonding temperature of 813 K, the amorphous oxide film was broken to small pieces, and also crystalline particles about 10-100 nm in size were dispersed. The broken amorphous oxide film and crystalline particle coexisted also at 833 K (Fig. 1 (c)). As can be seen from Figs. 1(b) and 1(c), crystalline particles were formed in areas where the amorphous oxide films disappeared. As shown in Figs. 1(d) to 1(f), no amorphous film could be observed at bonding temperatures of 843 K or higher. Thus, as the bonding temperature was increased, the crystalline oxide particle became dominant compared with the amorphous oxide film, and tended to be coarsened. The crystal structure of the oxide particle at the joint interface of the 6063 alloy was identified as Al_2MgO_4 by electron diffraction patterns at all the bonding temperatures employed[6]. This suggests that the morphological alteration of the interfacial oxide films to dispersed particles shown in Fig. 1 resulted from the crystallization of the amorphous oxide film.

The effect of bonding temperature on the morphology of the interfacial oxide of the 5005 alloy is shown in **Fig. 2**. The joint interfaces were also tilted by 35° to the incident beam. As the bonding temperature

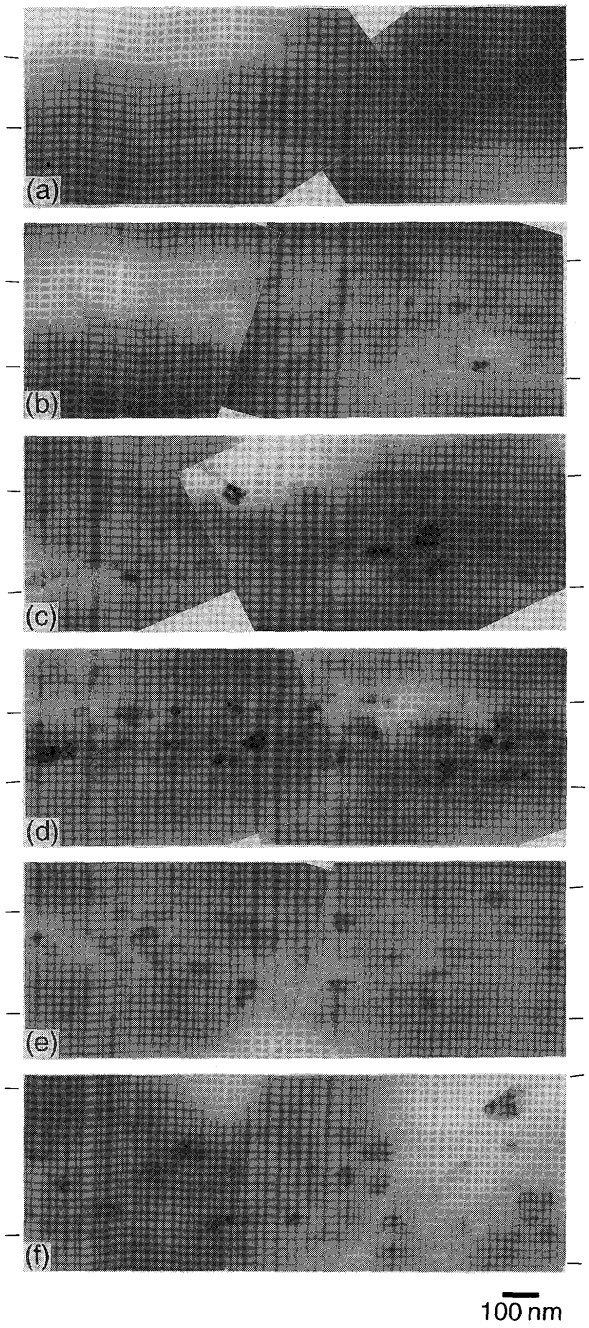

Fig. 1 Electron micrographs of bond interfaces of 6063 alloy tilted by 35° to the incident beam (T_W= bonding temperature, P_W=bonding pressure, and t_W=bonding time) : (a) T_W=793 K, P_W=4 MPa, (b)T_W=813 K, P_W=2MPa, (c) T_W=833 K, P_W=1 MPa, (d)T_W=843 K, P_W=1 MPa, (e) T_W=873 K, P_W=1 MPa, and (f) T_W=893 K, P_W=1 MPa .

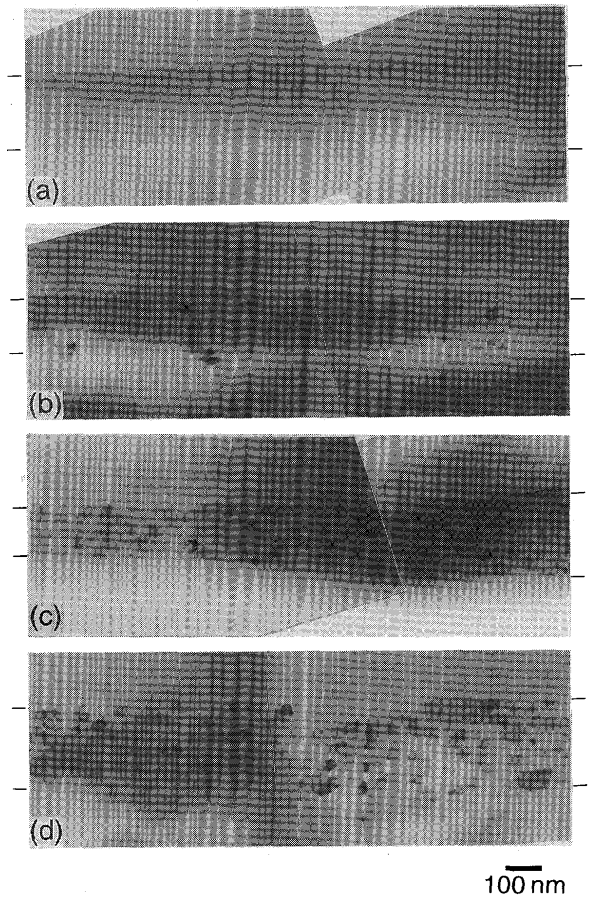

Fig. 2 Electron micrographs of bond interfaces of 5005 alloy tilted by 35° to the incident beam: (a) T_W=793 K, P_W=3 MPa, (b) T_W=813 K, P_W=2 MPa, (c) T_W=833 K, P_W=1 MPa, and (d) T_W=873 K, P_W=1 MPa

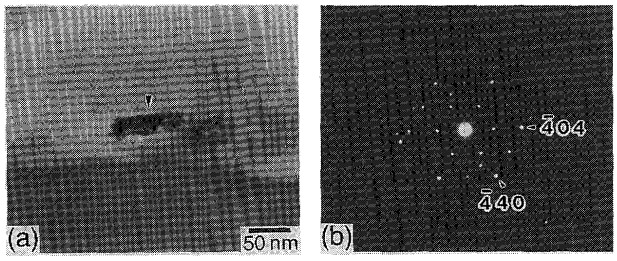

Fig. 3 (a) Enlarged micrograph of a crystalline oxide particle at the bond interface of 5005 alloy (T_W=873 K, P_W=1 MPa). (b) Electron diffraction pattern from the particle in (a) identified as Al_2MgO_4 (beam // [111] Al_2MgO_4).

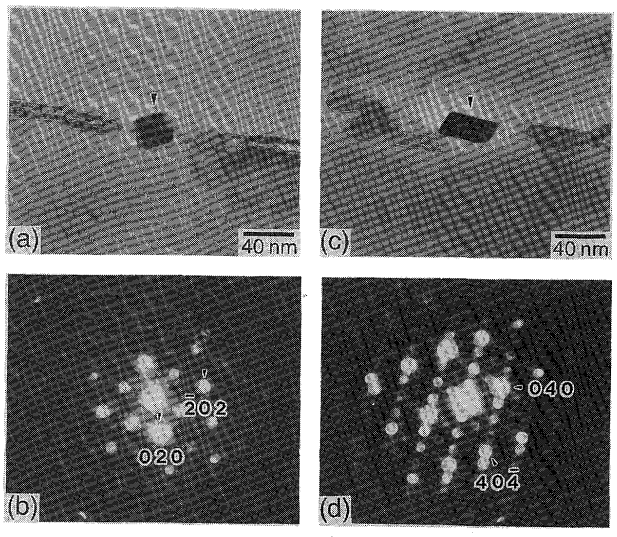

Fig. 4 (a),(c) Enlarged micrographs of crystalline oxide particles at the bond interface of 5005 alloy (T_W=813 K, P_W=2 MPa). (b) Electron diffraction pattern from the particle in (a) identified as MgO (beam // [101] MgO). (d) Electron diffraction pattern from the particle in (c) identified as Al_2MgO_4 (beam // [101] Al_2MgO_4).

was increased, the morphology of the interfacial oxide in the 5005 alloy joint was altered from amorphous films to crystalline particles 10-100 nm in size similar to that of the 6063 alloy joint, although the amorphous oxide film was annihilated at lower bonding temperatures. However, oxide particles of a crystal structure different from Al_2MgO_4 were also observed in this case. Oxide particles at the joint interface of the 5005 alloy bonded at 873 K (**Fig. 3(a)**) were identified as Al_2MgO_4 by SAD patterns as shown in Fig. 3(b). At a bonding temperature of 813 K, however, the oxide particles shown in **Figs. 4** (a) and 4(c) were identified as MgO and Al_2MgO_4 (see Figs. 4(b) and 4(d)), respectively. Thus, crystalline oxide particles of MgO and Al_2MgO_4 coexisted at the joint interface of 5005 alloy at bonding temperatures from 823 K to 833 K, and the Al_2MgO_4 particle became dominant with the rise in bonding temperature.

The effect of bonding temperature on the morphology of the interfacial oxide of the 7N01 alloy is shown in **Fig. 5**. The joint interfaces shown in Fig. 5 are also tilted by 35° to the incident beam. As shown in Fig. 5(a), almost all amorphous oxide films were broken to small pieces even at a bonding temperature of 733 K, while larger ones were observed at the joint interfaces of 5005 and 6063 alloys in this temperature range. The dispersed crystalline oxide particle was about 10-100 nm in size. At bonding temperatures above 763 K, only

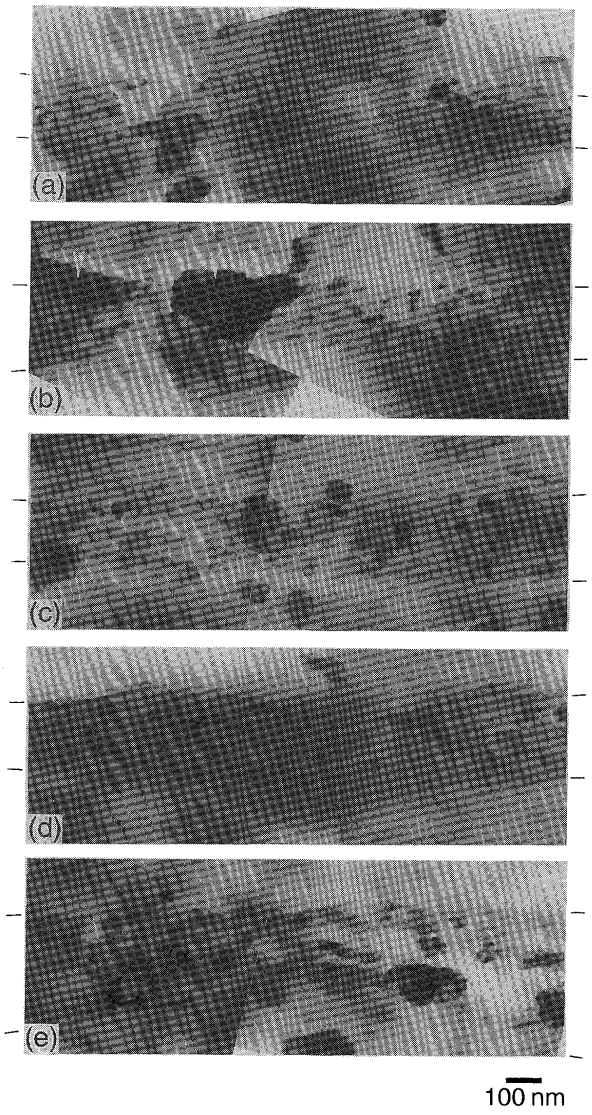

Fig. 5 Electron micrographs of bond interfaces of 7N01 alloy tilted by 35° to the incident beam: (a) T_W=733 K, P_W=6 MPa, (b) T_W=763 K, P_W=6 MPa, (c) T_W=793 K, P_W=5 MPa, (d) T_W=853 K, P_W=1 MPa, and (e) T_W=893 K, P_W=1 MPa

dispersed crystalline oxide particles were observed as can be seen in Figs. 5(b) to 5(e). Thus, the amorphous oxide film of the 7N01 alloy joint was annihilated at bonding temperatures much lower than those of the 6006 and 5005 alloy joints. The dispersed oxide particle was coarsened with the rise in bonding temperature as can be seen from Fig. 5. The crystal structure of the oxide particle at the joint interface of the 7N01 alloy was identified as MgO by electron diffraction analyses at all bonding temperatures employed. No coexisting

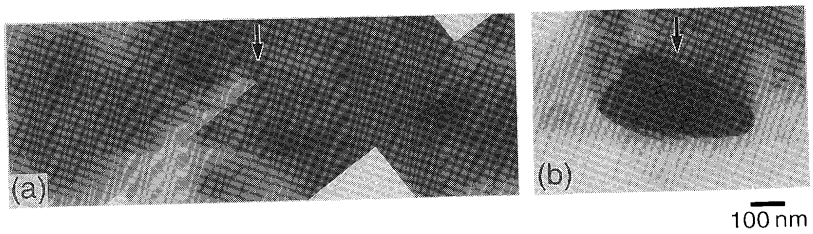

Fig. 6 (a) Electron micrographs of bond interfaces of 6063 alloy where continuous oxide film is vanished and the outline of precipitate Mg_2Si can be seen. Precipitate Mg_2Si in (a) is clearly observed in (b). (T_w=793 K, P_w=4 MPa).

Al_2MgO_4 particle was observed at the joint interface of the 7N01 alloy.

The ranges of bonding temperature and Mg content in which Al_2MgO_4 and MgO formed can be explained thermodynamically by assuming that these crystalline oxides were formed through the reductive reactions of the interfacial amorphous oxide film with Mg[9].

In addition to the interfacial oxide, large interfacial phases were observed in the 7N01 alloy joint as indicated by the arrow in Fig. 5(b). These interfacial phases can be regarded as precipitates formed preferentially at the joint interface. Crystalline particles 50-200 nm in size observed in the matrix can be regarded as relatively insoluble compounds, since Cr and Mn were detected in these particles by EDS analyses. Similar interfacial precipitates were also observed at the joint interface of 6063 alloy as shown in **Fig. 6**. The interfacial precipitate in the 7N01 alloy joint had a flat shape of 1-2 μm length and 0.2-0.5 μm thickness, and were observed at an interval of several μm. The dimensions of these interfacial phases and the intervals were almost independent of the bonding temperature, when the Al_2MgO_4 particle was predominant over the amorphous oxide film. By electron diffraction analyses, these interfacial phases were identified as Mg_2Si in the 6063 alloy joint and $MgZn_2$ in the 7N01 alloy joint. Since these metallic compounds are known as stable phases in the equilibrium phase diagrams, and the contents of Mg, Si, and Zn of these alloys are within the solubility limits at all bonding temperatures employed, the formation of Mg_2Si and $MgZn_2$ at the joint interface can be attributed to precipitation during the cooling process after diffusion bonding.

These precipitates Mg_2Si and $MgZn_2$ were formed preferentially at the joint interface even compared with the grain boundary. When the oxides of continuous amorphous film and crystalline particle coexisted at the joint interface of 6063 alloy, as shown in Fig. 6, Mg_2Si precipitates were observed only in areas where the crystalline particle of Al_2MgO_4 was formed; i.e., they could not be observed in the area where the amorphous oxide film remained. The similar tendency of the formation site of the Mg_2Si particle was also observed at higher bonding temperatures. These results suggest that the crystalline oxide particle of Al_2MgO_4 is a preferential nucleation site for the precipitation of Mg_2Si compared with the amorphous oxide film and the grain boundary.

The interfacial oxide and precipitate observed at the joint interfaces of the 6063, 5005, and 7N01 alloys are summarized in **Fig. 7**. In a previous paper [5], we have reported that the morphology and crystal structure of the

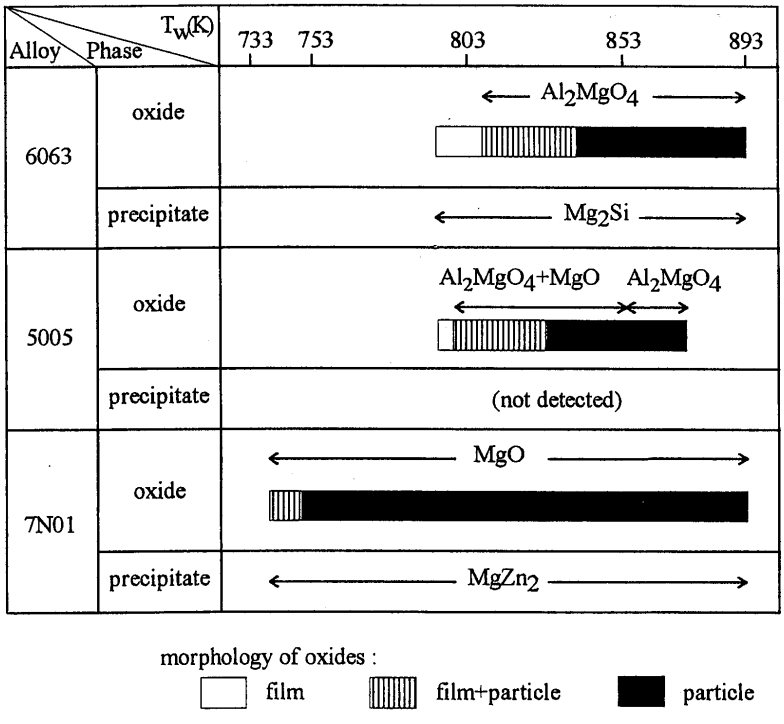

Fig. 7 Influences of the bonding temperature on the interfacial phases in the joints of 6063, 5005, and 7N01 alloys.

oxide at the joint interface of aluminum alloys depended on the Mg content of the alloy, when the bonding temperature was about 873K. Figure 7 shows that they depend on the bonding temperature as well and the amorphous film is altered to the crystalline particle at lower bonding temperatures, as the Mg content is increased.

3.2 Tensile strength of joints

The tensile strength of the 6063 alloy joint is shown as a function of bonding temperature in **Fig. 8**. The tensile strength increased from 40 MPa to 160 MPa, as the bonding temperature was increased from 793 K to 843K. In Fig. 8, the morphology of the interfacial oxides observed at various bonding temperatures is also shown for comparison. It should be noted that the substantial increase in the tensile strength and the annihilation of the amorphous oxide film occurred in almost the same temperature range, and the tensile strength became almost independent of the bonding temperature, when the amorphous oxide film was annihilated. The tensile strength of as-bonded joints, however, was lower than that of the base metal, and all of them were fractured at the interface in tensile tests.

In case of commercially pure aluminum 1080, the tensile strength of joints was much lower than that of 6063 alloy joints, and increased at higher bonding temperatures. As described in a previous paper [4], this is due to the continuous amorphous oxide film remaining at the joint interface even at high bonding temperatures close to the melting point.

The tensile strength of the 7N01 alloy joint is shown as a function of bonding temperature in **Fig. 10**. As the bonding temperature was increased, the tensile strength of the 7N01 alloy joint increased, and then decreased, passing through a maximum at 823-853 K. The significant increase in the tensile strength and the morphological change in the interfacial oxide were observed in almost the same temperature range. These results, shown in Figs. 8, 9, and 10, suggest that (1) the interfacial oxide film is a critical factor controlling the bond strength and (2) the crystalline oxide particles of Al_2MgO_4 and MgO have only slight influence on the bond strength compared with the amorphous oxide film. Thus, when there is no interfacial phase other than the oxide, its morphology is regarded as a major factor controlling the bond strength of the aluminum alloy joint.

However, the joints of 6063 and 7N01 alloys were fractured at the joint interface even when the bonding temperature was high enough to annihilate the amorphous oxide film. At the joint interfaces of these

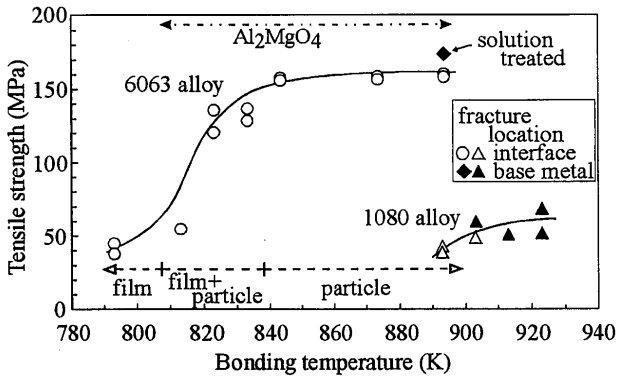

Fig. 8 Tensile strength vs. bonding temperature for joints of 6063 alloy and joints of commercially pure Al 1080.

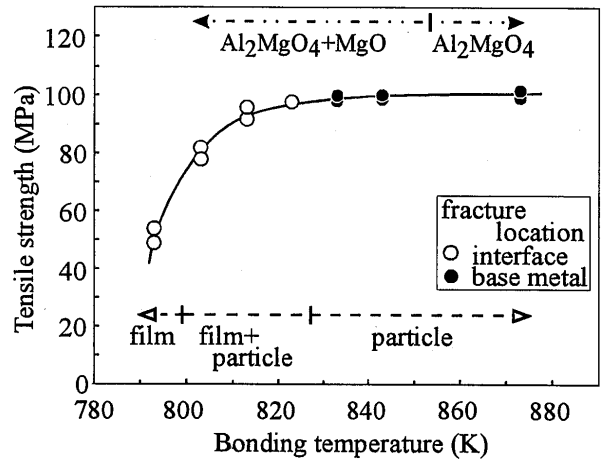

Fig. 9 Tensile strength vs. bonding temperature for joints of 5005 alloy.

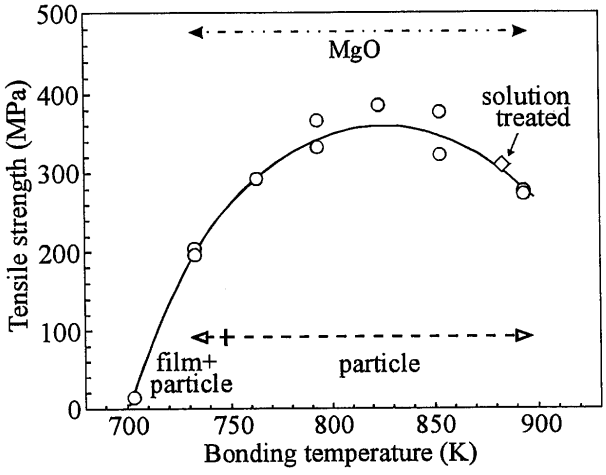

Fig.10 Tensile strength vs. bonding temperature for joints of 7N01 alloy.

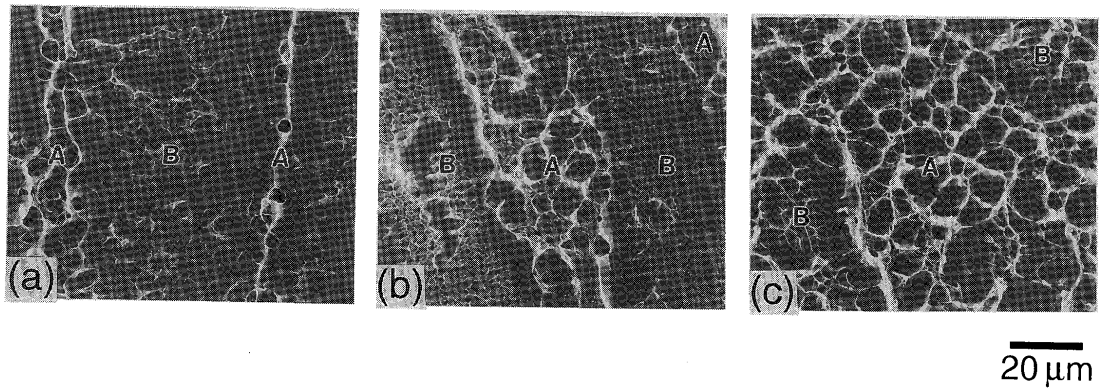

Fig. 11 Fractured surfaces of joint of 6063 alloy: (a) T_W=833 K, P_W=1 MPa, (b) T_W=873 K, P_W=1 MPa, and (c) T_W=893 K, P_W=1 MPa.

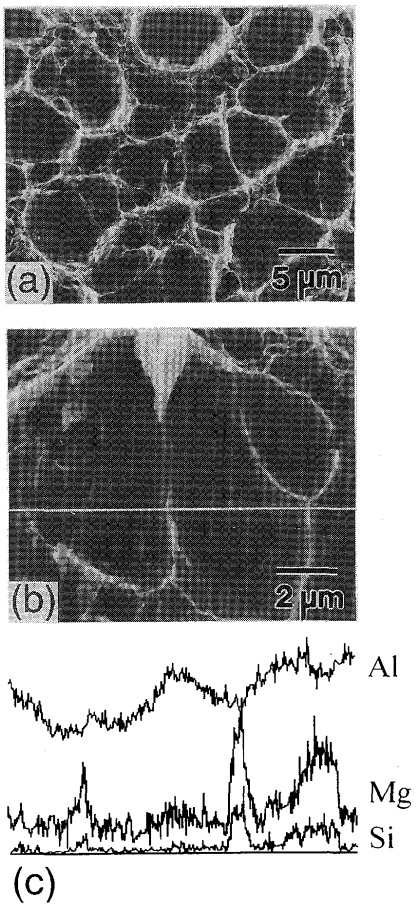

Fig. 12 Fractured surface of a joint of 6063 alloy showing large dimples at lower magnification (a) and at higher magnification (b). The intensity of characteristic X-rays of Al, Mg, and Si along the white line in (b) are shown in (c). (T_W=873 K, P_W=1 MPa).

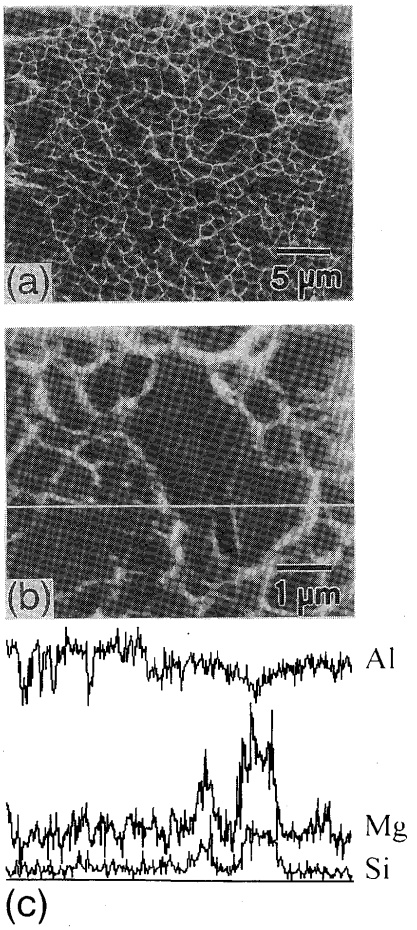

Fig. 13 Fratucred surface of a joint of 6063 alloy showing small dimples at lower magnification (a) andat higher magnification (b). The intensity of characteristic X-rays of Al, Mg, and Si along the white line in (b) are shown in (c) (T_W=873 K, P_W=1 MPa).

alloys, the precipitates of $MgZn_2$ and Mg_2Si occurred as shown in Figs. 5 and 6. In contrast, the joint of 5005 alloy in which no interfacial precipitate was observed were fractured at the base metal in a tensile test, when the amorphous oxide film was annihilated. These results suggest that the intermetallic compound precipitate at the joint interface also has a considerable influence on the bond strength.

A fractured surface of the 6063 alloy joint bonded at 833 K is shown in **Fig. 11**(a). On this fractured surface, two characteristic areas A and B were observed alternately along the trace of turning in a lathe. As shown in Fig. 11(a), areas A and B represented dimple patterns and rather flat appearance, respectively. At higher bonding temperatures, as shown in Figs. 11(b) and 11(c), small dimples appeared also in area B. As the bonding temperature was increased, dimples both in area A and in area B became larger and deeper, and the area fraction occupied by area A was increased. Detailed observations of the fractured surface of 6063 alloy joint was carried out in order to examine the nucleation site of the dimple. Areas A and B observed at higher magnification were shown in **Figs. 12** and **13** along with the EDS line analyses across large dimples. As can be seen in Fig. 12(a), area A consisted of large dimples of 3-5 μm diameter and finer dimples on the rim of the large dimples. As shown in Fig. 12(b), at the bottom of the large dimple a cracked interfacial phase of 3-5 μm diameter was observed in many cases. The contents of Mg and Si were increased at this interfacial phase as shown in Fig. 12(c), suggesting that this interface phase was a precipate of Mg_2Si which was observed with TEM (see Fig. 6). On the hand, as shown in Fig. 13 (a) in area B large dimples of 2-3 μm diameter were also observed among small dimples of about 1 μm diameter. At the bottom of this large dimple in area B, as shown in Fig. 13(b), a cracked interfacial phase of 2-3 μm diameter was also observed, which can be regarded as a Mg_2Si precipitate from the results of the EDS line analyses as shown in Fig. 13(c). The number densities of large dimples in area B approached that observed in area A, as the bonding temperature was increased. The number density of the large dimples observed in Figs. 12 and 13 was estimated to be $\sim 5 \times 10^{10}$ m^{-2}.

Thus the number density of the large dimple is nearly equal to that of Mg_2Si precipitates estimated from their average intervals (see Fig. 6). This suggests that the Mg_2Si precipitate acts as the nucleation site of the large dimple shown in Figs. 12 and 13. The distributions of the Al_2MgO_4 particles and Mg_2Si precipitates observed with TEM were schematically illustrated in

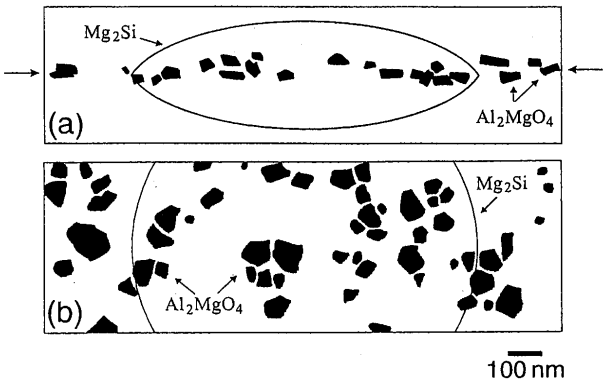

Fig. 14 Schematic representation of the distribution of Al_2MgO_4 and Mg_2Si on the bond interface of 6063 alloy. The bond interface is perpendicular (a) and parallel (b) to the page plane. (T_W=873 K, P_W=1 MPa).

Fig. 14. In Fig. 14, Mg_2Si was depicted in a lenticular shape of 1 μm diameter and 0.3 μm thickness. In Fig. 14(a), Al_2MgO_4 particles observed from a direction parallel to the interface are schematically illustrated, and their average projected length and height were assumed to be 50 nm and 20 nm from the results of TEM observations. Thus the crystalline particles of Al_2MgO_4 grew preferentially in the direction parallel to the joint interface. In a plan view, as shown in Fig. 14(b), no anisotropy in the shape of Al_2MgO_4 particle was found, and the average projected Heywood diameter was estimated to be about 50 nm. The number density of the Al_2MgO_4 particles on the joint interface was estimated

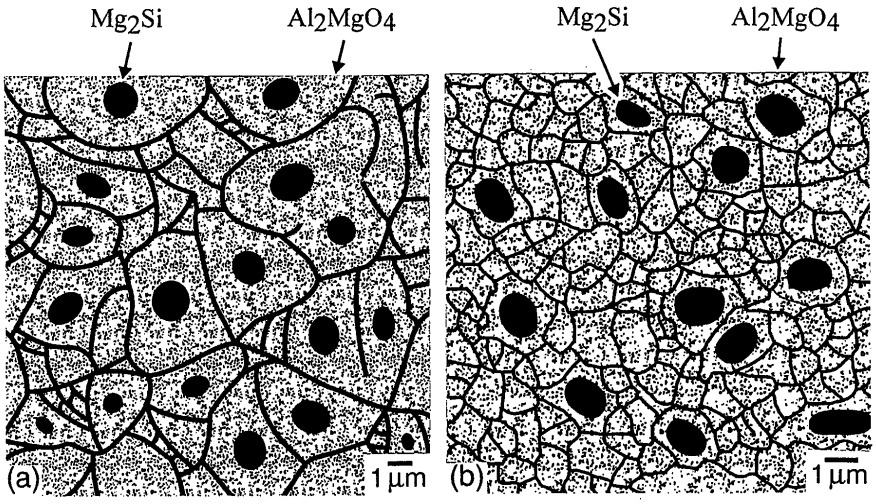

Fig. 15 Schematic representation of the distribution of oxide and precipitate on the fractured surface of a joint of 6063 alloy, where (a) and (b) show areas corresponding to Fig. 12(a) and Fig. 13(a), respectively.

to be ~10^{14} m^{-2}, although there might be uncounted Al_2MgO_4 particles because of the diffraction contrast of the TEM image depending on the crystal orientation. In **Fig. 15**, the schematic diagram of the distributions of the Al_2MgO_4 particle and Mg_2Si precipitate were superposed on those of the fracture morphologies observed in areas A and B. The geometrical relationships between the interfacial phases and the dimple patterns can be appreciated from Fig. 15.

In general, it has been said that the dimple pattern is formed through the nucleation of a microvoid in the vicinity of the second phase particles like precipitates and inclusions, and the following growth and coalescence of the microvoid. The precipitate of Mg_2Si was much larger than the Al_2MgO_4 particle, and was presumably fragile, as suggested by Figs. 12(b) and 13(b). Therefore, the Mg_2Si precipitate can be regarded as an effective initiation site of dimples. This supports the suggestion that the Mg_2Si precipitate was the nucleation site of the large dimple shown in Figs. 12(a) and 13(b). The fine dimple on the rim of the large dimple (see Fig. 12(a)) and that observed in area B were possibly nucleated by Al_2MgO_4 particles and coalesced.

When a considerable amount of the amorphous oxide film remained at the joint interface (bonding temperatures lower than 840 K), area A was narrower and area B exhibited rather flat appearance, as shown in Fig. 11(a). This suggests that the appearance of the fractured surface was strongly influenced by the amorphous oxide film remaining at the joint interface. At higher bonding temperatures (see Fig. 11(c)), area A occupied almost the whole fracture surface, suggesting that most dimples were initiated at the Mg_2Si precipitate. Therefore it can be considered that the effect of the Mg_2Si precipitate on the tensile strength became relatively important as the bonding temperature was increased.

In order to evaluate the effect of the Mg_2Si precipitate on the bond strength, a joint of 6063 alloy bonded at a high temperature (893 K) was subjected to the solution treatment for dissolving the Mg_2Si precipitate. The solution treatment consisted of holding for 7.2 ks at 793K and subsequent quenching into iced water. As shown in Fig. 8, while the as-bonded joint was fractured at the joint interface, the solution-treated joint was fractured at the base metal, and had tensile strength higher than the as-bonded joint by 15 MPa. It follows from this result that although the Mg_2Si precipitate acted as a nucleation site of dimple, its influence on the joint strength was not so strong as that of the amorphous oxide film.

Similarly, the tensile strength of a 7N01 alloy joint bonded at 883 K was also measured after the solution treatment. In contrast to the result of the 6063 alloy joint, the solution treatment was not effective in improving the tensile strength of the 7N01 alloy joint, and the solution-treated joint was fractured at the joint interface, as shown in Fig. 10. Since Al-Zn-Mg alloys are known to be subject to intergranular brittle fracture, it may be suggested that the presence of the MgO particle is more serious for the strength of the joint interface of the 7N01 alloy than the oxide particles in the 6063 and 5005 alloy joints. From these results, it can be concluded that the interfacial precipitates have only slight influences on the joint strength of the 6063 and 7N01 alloys compared with the amorphous oxide film, and the amorphous oxide film is the most important factor controlling the bond strength.

4. Conclusions

In order to investigate the factor controlling the strength of the diffusion-bonded joint of the aluminum alloy, the interfacial phase has been observed with TEM for the joints of commercial aluminum alloys, Al-Mg-Si alloy 6063, Al-Mg alloy 5005, and Al-Zn-Mg alloy 7N01, and compared with the tensile strength and fracture morphology of the joint. The results obtained are summarized as follows:

(1) At the joint interfaces of these alloys, amorphous oxide films were observed, and they were altered gradually to crystalline oxide particles, as the bonding temperature was increased. The amorphous oxide film disappeared at lower bonding temperatures, as the Mg content was increased.

(2) The crystalline oxides at the joint interfaces of the 6063 and 7N01 alloys were identified as Al_2MgO_4 and MgO, respectively. At the joint interface of the 5005 alloy, both Al_2MgO_4 and MgO were observed at bonding temperatures below 853 K, and only Al_2MgO_4 was observed above 853 K.

(3) Intermetallic compounds much larger than the crystalline oxide particles were precipitated preferentially at the joint interface even compared with the grain boundary. These precipitates observed in the joints of 6063 and 7N01 alloys were identified as Mg_2Si and $MgZn_2$, respectively.

(4) As the area occupied by the amorphous oxide film was decreased, the tensile strength of the joints of all the alloys increased significantly, suggesting that the amorphous oxide was a major factor that decreased the

bond strength. Although the fracture morphology of the joint suggested that the intermetallic compound precipitates acted as initiation sites of dimples in tensile test, their influences on the bond strength can be considered to be less significant than the amorphous oxide film.

References

1) T. Enjo, K. Ikeuchi, and N. Akikawa : Trans. JWRI, Vol. 10(1981), 45.
2) T. Enjo, K. Ikeuchi, and K. Furukawa : Trans. JWRI, Vol. 14(1985), 115.
3) T. Enjo, K. Ikeuchi, and H. Fujita : Trans. JWRI, Vol.15 (1986), 117.
4) T. Enjo, K. Ikeuchi, and H. Yoshikawa : IIW Doc. No. IX-1561-89, (1988).
5) K. Kotani, K. Ikeuchi, and F. Matsuda : IIW. Doc. No. IX-1797-95, (1995).
6) K. Ikeuchi, K. Kotani, and F. Matsuda : Quart. J. Japan Weld. Soc., Vol. 14(1996), 122.
7) K. Kotani, K. Ikeuchi, and F. Matsuda : Quart. J. Japan Weld. Soc., Vol.14(1996), 382.
8) T. Enjo, K. Ikeuchi, and T. Horinouchi : Trans. JWRI, Vol.15(1986), 61-68.
9) K. Kotani, K. Ikeuchi, and F. Matsuda : Quart. J. Japan Weld. Soc., Vol.14(1996), 551.